Journal of Contaminant Hydrology 136-137 (2012) 10–24

Contents lists available at SciVerse ScienceDirect

Journal of Contaminant Hydrology

journal homepage: www.elsevier.com/locate/jconhyd

# Laboratory investigations of the effects of geologic heterogeneity on groundwater salinization and flush-out times from a tsunami-like event

M. Vithanage [a,b,c,*], P. Engesgaard [a], K.H. Jensen [a], T.H. Illangasekare [d], J. Obeysekera [e]

[a] Department of Geography and Geology, University of Copenhagen, Øster Voldgade 10, 1350 Copenhagen, Denmark
[b] International Water Management Institute, Battaramulla, Sri Lanka
[c] Chemical and Environmental Systems Modeling Research Group, Institute of Fundamental Studies, Hantana Road, Kandy, Sri Lanka
[d] Center for Experimental Study of Subsurface Environmental Processes, Department of Civil and Environmental Engineering, Colorado School of Mines, Golden, CO, USA
[e] Department of Hydrologic and Environmental Systems Modeling, South Florida Water Management District, West Palm Beach, FL, USA

ARTICLE INFO

*Article history:*
Received 23 March 2011
Received in revised form 28 April 2012
Accepted 8 May 2012
Available online 12 May 2012

*Keywords:*
Shallow coastal sandy aquifers
Variable density flow
Solute transport
Saltwater

ABSTRACT

This intermediate scale laboratory experimental study was designed to improve the conceptual understanding of aquifer flushing time associated with diffuse saltwater contamination of coastal aquifers due to a tsunami-like event. The motivation comes from field observations made after the tsunami in December, 2004 in South Asia. The focus is on the role and effects of heterogeneity on flushing effectiveness. A scheme that combines experimentation in a 4.8 m long laboratory tank and numerical modeling was used. To demonstrate the effects of geologic heterogeneity, plume migration and flushing times were analyzed in both homogeneous and layered media and under different boundary conditions (ambient flow, saltwater infiltration rate, freshwater recharge). Saltwater and freshwater infiltrations imitate the results of the groundwater salinization from the tsunami and freshening from the monsoon rainfall. The saltwater plume behavior was monitored both through visual observations (digital photography) of the dyed salt water and using measurements taken from several electrical conductivity sensors installed through the tank walls. The variable-density, three dimensional code HST3D was used to simulate the tank experiments and understand the fate and movement of the saltwater plume under field conditions. The results from the tank experiments and modeling demonstrated that macro-scale heterogeneity significantly influenced the migration patterns and flushing times of diffuse saltwater contamination. Ambient flow had a direct influence on total flush-out time, and heterogeneity impacted flush-out times for the top part of the tank and total flush-out times. The presence of a continuous low-permeability layer caused a 40% increase in complete flush-out time due to the slower flow of salt water in the low-permeability layer. When a relatively small opening was introduced in the low-permeability layer, salt water migrated quickly into a higher-permeable layer below causing a reduction in flush-out time. Freshwater recharge caused an early dilution of salt water in the top part of the tank in the case of a layered media, but also pushed the saltwater plume into the low-permeability layer which led to increased total flush-out times.



## 1. Introduction

The 26th December 2004 tsunami in Southeast Asia caused widespread contamination of coastal aquifers across the southern Asian countries by seawater flooding and infiltration. In the eastern coastal belt of Sri Lanka groundwater is the only source of freshwater. The resource often

* Corresponding author at: Chemical and Environmental Systems Modeling Research Group, Institute of Fundamental Studies, Hantana Road, Kandy, Sri Lanka. Tel.: +94 812232002; fax: +94 812232131.
*E-mail address:* meththikavithanage@gmail.com (M. Vithanage).

0169-7722/$ – see front matter © 2012 Elsevier B.V. All rights reserved.
doi:10.1016/j.jconhyd.2012.05.001

occurs as freshwater lenses lying on top of salt water between the sea and inland brackish water lagoons. In these areas the tsunami inundation extended up to 3 km inland in some places, flooding and damaging about 40,000 shallow dug wells used for domestic water supply in Sri Lanka alone (Illangasekare et al., 2006; Vithanage et al., 2009).

The protection and management of freshwater lenses in coastal aquifers (barrier islands, atolls) is of great interest because they appear worldwide (see e.g. Vithanage et al., 2009). A tsunami flooding of these areas has a severe impact on groundwater resulting in salinization of the freshwater lens making coastal aquifers unusable until salinity is reduced to potable concentrations. Knowing how long it takes to return to the preexisting conditions is critical for the management of the groundwater resource. The tsunami occurred in the wet season (monsoon) on the eastern coastal belt of Sri Lanka, when the water table was highest (shallow unsaturated zone) and with a mounding between the lagoon and sea approximately coinciding with the maximum inundation distances (Vithanage et al., 2009). An enhanced downward infiltration is expected due to the very high inundation depth of the denser salt water created by the tsunami flood. The macro-scale heterogeneity in the form of sand and clay layers in the subsurface can cause more complex saltwater migration patterns, compared to homogeneous formations. For example, undersaturated conditions, layers of higher hydraulic conductivity may generate lateral preferential flow paths, and heterogeneity may also introduce the onset of gravitational instabilities as observed in laboratory experiments (Schincariol and Schwartz, 1990).

Carlson et al. (2008) and Vithanage et al. (2009) discussed point contamination of aquifers from storm surges and the 2004 tsunami through broken well pipes or open dug wells. However, there appear to be very few studies on the transient effects of flooding of seawater on diffuse salinization of groundwater. Anderson and Lauer (2008) investigated the role of over-wash events on increases in total dissolved solids (TDS) in a number of inland wells. The over-wash was created by a storm surge caused by a hurricane. They applied the two-dimensional density-dependent flow and transport model SUTRA and found that the plume penetration depth was sensitive to hydraulic conductivity, which was held constant and uniform in the model domain. The model predicted that it would take more than 10 years to flush out the saline plume from the two-day long over-wash event. However, the effect of heterogeneity was not included in the analysis. Andersen et al. (2005) reported on the effects of a small storm on the geochemical processes of a sinking saltwater plume in a shallow unconfined aquifer. The sinking of the plume continued for 49 days before reaching the aquifer bottom even though the storm only lasted for one day.

It is important to know what processes cause dilution of salt water after a tsunami event and how they control the time needed for flushing out salt water (referred to as "*plume flushing time*" hereafter) thereby reestablishing coastal aquifers as a source for potable water supply. These processes are related to the dynamics of the tsunami event itself (wave height and duration of ponding), land surface topography, hydrogeology of the aquifer (geological settings and hydraulic properties), flow patterns created by the infiltration (stable or unstable flow), and boundary conditions.

Several tank experiments on variable-density flow and transport have been reported in the literature. Many of these have used artificial, porous media-like glass beads (Oostrom et al., 1992a; Schincariol et al., 1993; Swartz and Schwartz, 1998) and have focused mainly on instabilities (Oostrom et al., 1992b; Schincariol and Schwartz, 1990; Simmons et al., 2002; Swartz and Schwartz, 1998). Other studies have used numerical modeling to examine the propagation of dense leachate plumes and to understand the hydrodynamics of density-driven flow and transport (Fan and Kahawita, 1994; Hayworth, 1993; Koch and Zhang, 1992; Liu, 1995; Liu and Dane, 1996; Post and Simmons, 2010; Prasad and Simmons, 2003; Simmons and Narayan, 1997; Simmons et al., 1999; Wooding et al., 1997a, 1997b). These studies mostly considered point sources and mainly focused on the onset of gravitational instabilities and found that they can be caused by both micro-heterogeneity and density differences. Different numerical codes have been used for these studies including SUTRA (Voss, 1984), MOCDENSE (Sanford and Konikow, 1985), HST3D (Kipp, 1987), FEFLOW (Diersch, 1988), MOCDENS3D (Oude Essink, 1998), and SEAWAT-2000 (Langevin and Guo, 2006). Numerical difficulties are inherent to the (unstable) variable-density flow and transport problem. The relative density difference, horizontal hydraulic conductivity, anisotropy ratio, and longitudinal and horizontal dispersivities all influence plume stability (Simmons and Narayan, 1997). For example, Koch and Zhang (1992) showed that low dispersivity values can produce gravitational instabilities at the bottom of the plume, while larger dispersivity values can increase plume stability. Schincariol et al. (1993) reported that the instabilities are due to numerical errors and these errors are difficult to control. However, with few exceptions previous work on unstable flow has not been related to tsunami or storm-surge events, but focused on point injections of e.g. leachate contamination (Guvanasen and Volker, 1983; Oostrom et al., 1992a, 1992b; Schincariol and Schwartz, 1990). Only few studies have considered diffuse contamination (Terry and Falkland, 2010; Wooding et al., 1997a, 1997b). Thus, more investigations are needed to fully understand the nature of variable-density flow and transport associated with diffuse contamination of aquifers due to events such as a tsunami, where large volumes of higher density fluids are applied over large areas.

The main objective of this study was to improve the conceptual understanding of the effects of geological heterogeneity (homogeneous versus layered) and rainfall recharge on saltwater plume migration and flush-out times after a sudden groundwater salinization event such as a tsunami. As a fundamental study of the processes is not possible in field settings due to lack of control and the infeasibility to fully characterize subsurface heterogeneity, a scheme that combines experimentation in an intermediate-scale (4.8 m long) laboratory tank and numerical modeling was used. Synthetic aquifers with known soil parameters were created and the ambient groundwater flow and application rates of saline and freshwater were controlled. The propagation of the saltwater plumes was monitored visually using dyes, and quantitative data on salinity concentrations were collected using automated sensors and aqueous grab sampling. The intermediate scale tank experiments reported in this paper were carried out using quartz sands as the porous medium under different boundary conditions and water application scenarios using; (i) an elongated saltwater source at the surface mimicking a tsunami that contaminates the groundwater, (ii) ambient flow as a freshening mechanism, and (iii) freshwater flux at the top of the water table mimicking the flushing and freshening effects from rainfall infiltration. The variable-density flow and transport model, HST3D, was used to simulate the tank experiments and specifically simulate flush-out times on the basis of the laboratory experiments using a consistent set of parameter values and boundary conditions. The modeling was not a validation exercise as the number of scenarios that were experimentally simulated was not adequate to achieve this; rather the model analysis allowed us to analyze the basic processes occurring during the movement of dense salt water in a heterogeneous subsurface environment and during the subsequent flushing by infiltrating freshwater.

## 2. Experimental methodology

A flow tank with dimensions of 4.8 × 0.05 × 1.2 m was used to physically model the density driven flow in homogeneous and heterogeneous saturated porous media. The tank walls were constructed with stiff aluminum frames lined with Plexiglas for visual observations (Barth et al., 2001). The experiments were performed using pre-sieved sand from Unimin Corporation, Emmett, Idaho, USA. Two different sand types were used (hereafter referred to as #30 and #70, with #30 being the coarse sand). Grain sizes ($d_{50}$) of #30 and #70 sands are 0.5 and 0.2 mm, respectively (Sakaki and Illangasekare, 2007).

Three different aquifer packing configurations were used in the physical simulations; one with a homogeneous medium (#30 sand) and two with different cases representing layered media (#70 sand embedded in #30 sand) (Fig. 1). The first heterogeneous packing configuration consisted of one continuous (3.75 m long and 0.15 m high) less permeable layer of #70 sand in the middle of the tank (Fig. 1). In the second heterogeneous packing configuration, the low-permeability layer had a 0.6 m long opening in the middle (Fig. 1) allowing the saltwater plume to preferentially enter the zone below. The configuration with the continuous low-permeability layer will be referred to as 'layered experimental configuration I' and the experiments with the discontinuity in the low-permeability layer will be referred to as 'layered experimental configuration II'.

All experiments were carried out as illustrated in Fig. 1 and are in some ways similar to the experiments presented by Zhang et al. (2002). Fresh tap water was supplied to the inflow head chamber (indicated by (1) in Fig. 1) from the plastic container (2), using a submersible pump, and water was allowed to leave the tank through the effluent chamber. The hydraulic head difference in the tank was controlled by adjusting the water levels in the two chambers. The gravel packed sections at both ends (3) buffered the effect of inflow and outflow by redistributing the flow across the porous medium. Porous stainless steel plates kept the sand from entering the reservoirs. The tank was packed wet with the mechanically sieved quartz sand in 5 cm increments to reduce air entrapment during packing. Tank walls were tapped frequently and sand was disturbed by stamping with a pointed stick to minimize layering. The outflow from the tank was discarded through a collection container (6).

Saline water for the experiments was prepared by dissolving non-iodized table salt with normal tap water (electrical conductivity (EC) ~ 0.5 mS/cm) until it reached an EC value of 56 mS/cm (35 ppt) and a density of 1025 kg/m$^3$ (20 °C), corresponding to sea water in the Indian Ocean. In all experiments the density of the saline water was kept constant.

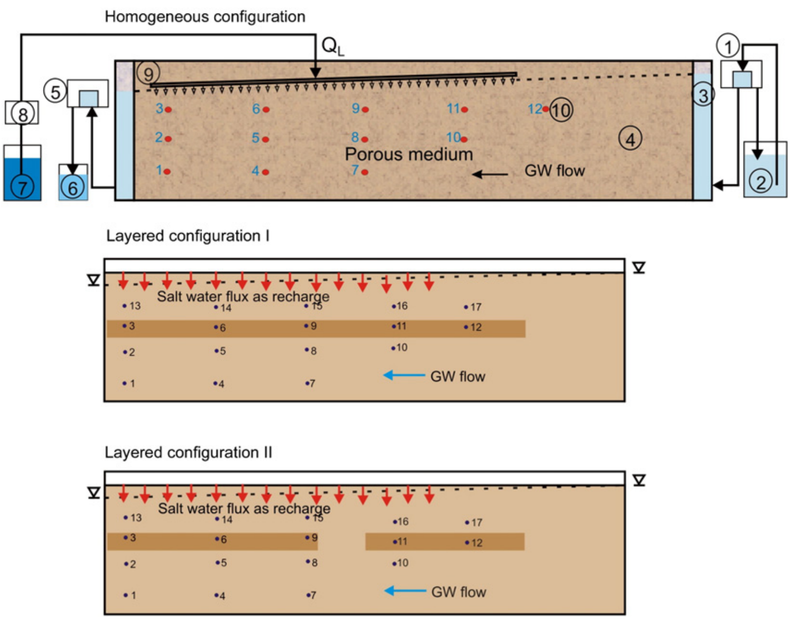


**Fig. 1.** (top) Experimental set up for homogeneous experiments: (1) inflow head chamber, (2) water storage tank, (3) gravel pack, (4) homogeneous porous media, (5) outflow head chamber, (6) waste water storage, (7) saltwater container, (8) peristaltic pump, (9) saltwater injection system and (10) electrical conductivity sensors; (middle) layered experimental configuration I; and (bottom) layered experimental configuration II. The light and dark brown areas correspond to sand #30 and #70, respectively. The locations of sensors are shown by numbers. (For interpretation of the references to color in this figure legend, the reader is referred to the web version of this article.)

The saltwater solution dyed with a red food color was stored in a container (7). A green food color was added to the freshwater used for recharge, which was applied in some of the experiments following the application of salt water. The red and green colors allowed for visual observation and digital photography. These food colors were non-sorbing to the silica sand and non-reactive with the Plexiglas (Goswami and Clement, 2007). The same concentration of food color was applied in all experiments to secure the same coloring conditions.

The saltwater flux was applied at the top of the tank at a constant rate over a given time period using 10 pressure-compensated rain dripper systems each consisting of 10 drippers and with 1 cm and 2 cm spacing between the drippers and dripper systems respectively (9). The rain dripper system was embedded immediately below the water table to avoid any interaction with the unsaturated sand. The drippers were driven by a peristaltic pump (Ismatic BVK 78006) (8). The flux application length was 2.8 m. The applied saltwater flux rate was kept sufficiently low to prevent ponding at the surface and the rate was kept constant throughout the application time. A drain tube with small conveyance loss was connected to the container near the tank outflow to allow discharge of the accumulated mixture of salt- and freshwater in the outflow chamber. This was found to be necessary to avoid changes in the head at the outlet reservoir.

The front movement of the saline plume was monitored using pre-calibrated $ECH_2O$-TE conductivity sensors (Decagon Devices Inc., WA, USA; location 10 in Fig. 1). The sensors were installed at predefined locations concurrently with the packing of the tank and connected to an automatic data logging unit (Campbell CR10X data logger and Decagon EM50). Small sampling tubes were placed at the sensor locations to extract aqueous samples for measurement of salinity for intermittent re-calibration of the automated sensors. The data obtained from the sensors were converted into concentrations using the procedure given in the manual of the $ECH_2O$-TE conductivity sensor. These sensors were selected because of their slim size thus minimizing the disturbance of flow and due to their ability to acquire high frequency data during the plume movement. However, during the progress of the experiments it was discovered that they are not designed to measure high saline concentrations near that of seawater and therefore the data exhibited significant noise (typically for concentrations higher than 8 ppt). Even with this shortcoming, the sensors provided time-continuous data to understand the trends in the dynamics of the plume migration. It was not practical to use grab samples to capture the spatial and high-frequency temporal variation of concentrations within the tank. To make most benefit of the data, several noise reduction techniques were investigated to obtain representative concentrations. Comparison of sensor calibration data and manual samples collected in some of the experiments showed that the best results for the breakthrough curves were obtained using the 90th percentile of the EC sensor data within a moving sampling window of 10 min. The oscillation in concentration data was inversely proportional to the length of the time window; however, overly large time windows produced too much smoothing that masked the real physical processes occurring in the system. Salinity values below 8 ppt were fairly stable; thus, the median values of the sub-sample were used when the observations fell below this threshold.

In total, 12 and 17 sensors were placed in the tank in the homogeneous and layered configurations I and II, respectively, with the extra 5 sensors installed in the low-permeability layer. During the layered experiments, manual samples were also drawn from the porous medium at a few of the sensor locations and conductivity (related to salinity) measured using Oakton CON100 handheld EC meter. The grab sampling was carried out every half hour during the first 6 h of the experiment and then at one-hour intervals. The plume configuration was also monitored using digital photographs every 30 min during the first 6 h and then every hour until the plume completely vacated the tank. Plume outlines were drawn by digitizing the boundaries of the color contrast at the edges of the plumes, which were clearly visible on the high-resolution photographs.

The hydraulic conductivities of the sands were determined by column experiments (one column for each sand and three replicates) giving values of $1.2\times10^{-3}$ and $1.4\times10^{-4}$ m/s for #30 and #70 sands, respectively, close to previously reported values for the same sand types (Sakaki and Illangasekare, 2007). A porosity of 0.43 was estimated gravimetrically for both sand types also close to the value of 0.41 reported by Sakaki and Illangasekare (2007).

After packing the tank, a tracer experiment was performed in the homogeneous configuration as in Goswami and Clement (2007) to ensure that the packing was uniform. Water soluble food dye injected through the inflow chamber resulted in a uniform migration with a sharp front. This indicated that the packing was uniform, and that solute transport was characterized by a low value of longitudinal dispersivity. The longitudinal dispersivity ($\alpha_L$) was not estimated directly from the experiment, instead, estimates from similar experiments (e.g. Frippiat et al., 2008; Moazed et al., 2009; Oswald and Kinzelbach, 2004) were used as initial values in the numerical modeling.

Five experiments were carried out for each tank configuration (Table 1). One of the five experiments included a freshwater loading event after application of salt water to represent infiltrating rain water. The freshwater infiltration event was created for a period of 1 h starting 1 h after the end of the saltwater application. Other boundary conditions that were varied in the experiments included the rate of saltwater recharge, the duration of saltwater application, and the ambient freshwater flow rate controlled using the heads in the end reservoirs.

## 3. Numerical model

The computer code HST3D (Kipp, 1987) was used to analyze the experimental data with the purpose of: (i) evaluating how effectively we can apply such tools to understand systems under controlled conditions with the aim to use these for simulating real events (Vithanage, 2009) and (ii) to simulate flush-out times on the basis of the laboratory experiments using a consistent set of parameter values and boundary conditions. The latter was important because the experiments were not carried out under exactly the same conditions (e.g. different hydraulic conductivities due to packing). The model is capable of simulating 3D flow, heat, and solute transport in variable-density flow systems. The ability to use several numerical schemes for weighting in space and time is important feature of this code as

**Table 1**
Details of experimental conditions. The flux application length is 2.80 m in all experiments.

| Experimental configuration | Exp. # | Salt water flux/area ($10^{-5}$ m/s) | Injection duration (h) | Head drop (m) | Freshwater flux | Time (h) |
|---|---|---|---|---|---|---|
| Homogeneous | 1.1 | 4.0 | 2.0 | 0.057 | | |
| | 1.2 | 4.0 | 2.0 | 0.085 | | |
| | 1.3 | 4.0 | 1.0 | 0.085 | | |
| | 1.4 | 5.3 | 1.0 | 0.085 | | |
| | 1.5 | 4.0 | 1.0 | 0.085 | √ | 1.0 |
| Layered 1 | 2.1 | 4.0 | 1.0 | 0.085 | | |
| | 2.2 | 2.6 | 1.0 | 0.065 | | |
| | 2.3 | 2.6 | 2.0 | 0.065 | | |
| | 2.4 | 2.6 | 2.0 | 0.085 | | |
| | 2.5 | 2.6 | 2.0 | 0.085 | √ | 1.0 |
| Layered II | 3.1 | 2.6 | 1.0 | 0.10 | | |
| | 3.2 | 4.0 | 1.0 | 0.10 | | |
| | 3.3 | 4.0 | 2.0 | 0.10 | | |
| | 3.4 | 4.0 | 2.0 | 0.085 | | |
| | 3.5 | 4.0 | 2.0 | 0.10 | √ | 1.0 |

the numerical accuracy can greatly influence the simulations of density-driven flow. The primary limitations are the long computing times and storage requirements necessary when using a high-resolution mesh to simulate variable-density flow. To save computational memory and time, the length of the solution domain was reduced to 4.0 m, while the width (0.05 m) and depth (1.1 m) were kept the same as in the tank. This reduction in the model domain was justifiable since the saline water flux in the flow container was applied away from the right boundary (Fig. 1) and the use of only 4.0 m in domain length would thus not affect the simulation of the salt plume. The specified boundary conditions were in the form of prescribed heads at the two sides, a dynamic flux boundary at the top and no flow boundary at the bottom. At inflow boundaries, the concentration of the incoming water was specified, while a zero concentration gradient was assumed at outflow boundaries.

Plume instabilities may arise due to many factors in variable-density flow simulations. Numerical dispersion (grid-dependent smearing of sharp solute concentration fronts) and oscillation (overshooting and undershooting of true solution) are well known difficulties in simulating advection-dominated solute transport phenomena (Diersch and Kolditz, 2002). In variable-density simulations, these effects can artificially generate a different movement of salt water.

The coupled flow and transport equations were solved using Picard iteration and backward-in-time, central-in-space finite difference schemes. A sensitivity test on grid size showed that a uniform grid of 0.5 cm in both directions provided acceptable accuracy, satisfying the range of Peclet numbers suggested by Huyakorn and Pinder (1983). For specified dispersivity values and the given cell sizes, the Peclet number was estimated to be between 2.5 and 10. During saltwater injection when vertical transport is of significance, the Peclet number in vertical direction may be 10 or higher. We realize that the common Peclet criterion was violated at times; however, the sensitivity analysis showed that the effect on the predicted plume flushing times was insignificant. The Courant criterion was used to select an appropriate time step giving computer run times of ~48 h. The maximum overshoot in scaled mass fraction for the entire simulation was 1.045, which occurred in <25 nodes out of about 350,000 nodes used in the simulation. This overshoot might have caused additional local instabilities as discussed below. A grid convergence test with a coarser (2 cm), medium (1 cm) and the applied fine mesh (0.5 cm) did not show a significant effect on plume migration time; however, the 2 cm and 1 cm meshes showed different plume behaviors (more stable likely as a result of added numerical dispersion) than what was observed from the photographs. Consequently, the fine mesh was considered adequate for determining plume migration and flush-out times.

The porous medium configurations were represented in the model by specifying a zone-based permeability for each sand type. Vithanage (2009) performed a model analysis of saltwater migration in the tank based on a stochastic representation of the centimeter-scale variability in permeability inside each zone. Although these simulations seemed to better match the randomness in the plume movement, they did not significantly change the simulated flush-out times. We did not include these simulations since a primary objective was to understand the effect of a layered media on flush-out time after a tsunami-like event and to compare situations with and without freshwater recharge.

## 4. Results: experimental observations

A total of 15 experiments were performed to examine the behavior of the saltwater plume (Table 1). Only a subset of these experiments was presented and discussed (but not in the order shown in the table). Common to all experiments was the generation of instabilities during the experiment (Fig. 2). To begin with, salt water enters the tank as distinct small plumes from each dripper. Relatively quickly the small plumes coalesce and one stable plume was generated in all experiments. After saltwater injection stopped, small gravitational instabilities (fingering) occurred at the bottom of the plume indicating unstable flow. Lobe-shaped protuberances formed first along the bottom edge of the plume and later within the plume. A similar finding was reported by Schincariol and Schwartz (1990). The degree of plume instability increased with decreasing ambient flow ($q_x$), which was also found by Oostrom et al. (1992a). Although the fingering was observed through the transparent back wall of the tank, the position, shape and time of appearance of the instabilities were slightly different at the

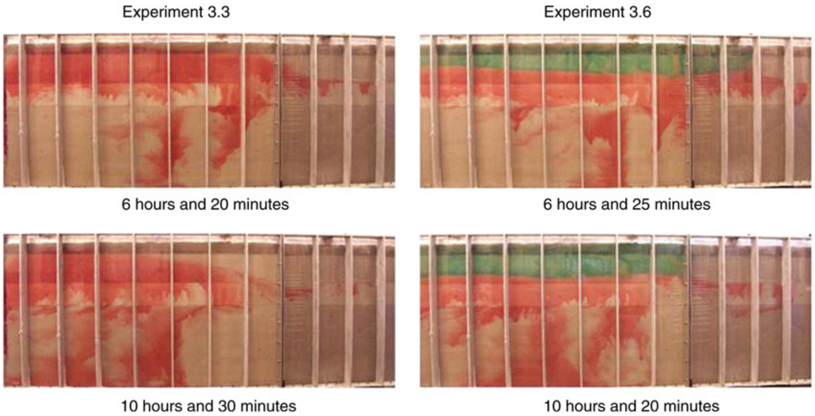


**Fig. 2.** Actual photograph of plume migration for layered Experiments 3.3 (left, no freshwater recharge) and 3.5 (right, freshwater recharge).

front wall. This indicated that the plume was three dimensional in nature, even though the thickness of the tank was considerably smaller than the other dimensions of the system. Schincariol and Schwartz (1990) and Oostrom et al. (1992a, 1992b) reported similar findings.

### 4.1. Homogeneous media

The configurations of plume migration are shown at different times during Experiments 1.3 (no freshwater recharge) and 1.5 (with freshwater recharge) in Fig. 3 (middle and right panes). The denser saltwater plume exhibited a rapid and relatively deep penetration into the sand. In Experiment 1.5, the freshwater remained on top of the saltwater plume. Application of freshwater pushed the saltwater plume further towards the base of the tank leading to slightly longer flush-out times. While the dense saltwater plume was subject to instabilities (see also discussion later), the neutral plume exhibited a stable and sharp interface. The introduction of freshwater after salt water imitating rainfall after the tsunami reduced the formation and the persistence of the gravitational instabilities in the saltwater plume.

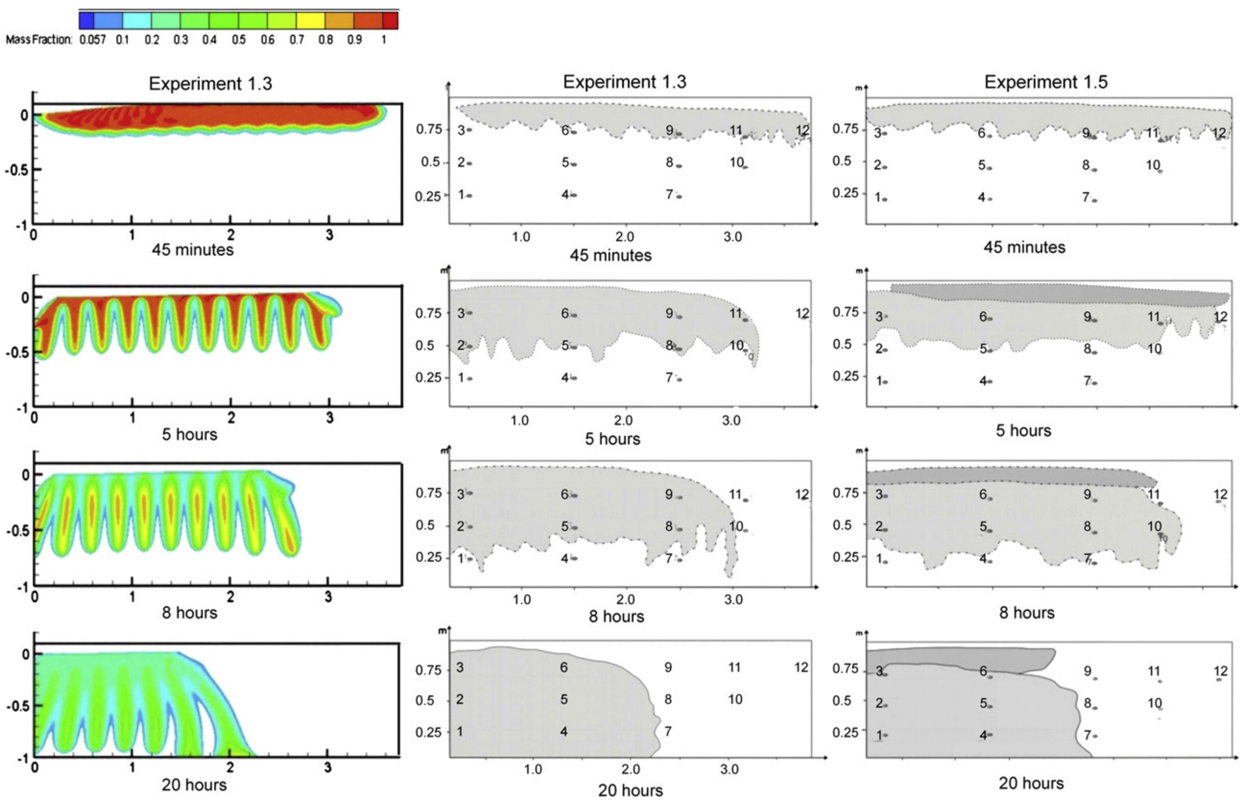


**Fig. 3.** (a) Simulations of Experiment 1.3, (b) digitized outlines of plume migration for Experiment 1.3, (c) digitized outlines of plume migration for Experiment 1.5. Light and dark gray areas represent saltwater and freshwater plumes, respectively.

Experiments 1.1 and 1.2 examined the generation and spreading of the saltwater plume as a function of ambient flow (results not shown). In these and other experiments, the plume initially moved downward and even slightly against ambient flow and towards the upstream end of the tank due to mounding. After a while, the entire plume began moving towards the downstream end in the direction of the ambient flow. As expected, migration time decreased as the head difference increased. The tank returned to initial conditions approximately 29% more quickly in Experiment 1.2 than in 1.1 as the head difference over the tank was increased from 0.057 to 0.085 m (32% increase). An increase of saltwater flux by 33% was simulated in Experiments 1.3 and 1.4 (Table 1), which leads to an increase in flushing time of ~5 h (not shown).

## 4.2. Layered media

Experiments 2.3 and 2.4 (Fig. 4) demonstrated the different plume migration patterns in layered experimental configuration I as caused by a change in the head difference from 0.065 m to 0.085 m. After the initial movement of the saltwater plume in the upper coarser sand layer, the plume reached the low-permeability layer and began accumulating on the interface and slowly penetrating into the low-permeability layer. Fingers developed upon entry into the low-permeability layer caused by the lower ambient flow velocity in this layer thus promoting free convection. The plume entered the underlying coarser sand layer as larger fingers, but formed a rather smooth interface first. With time,

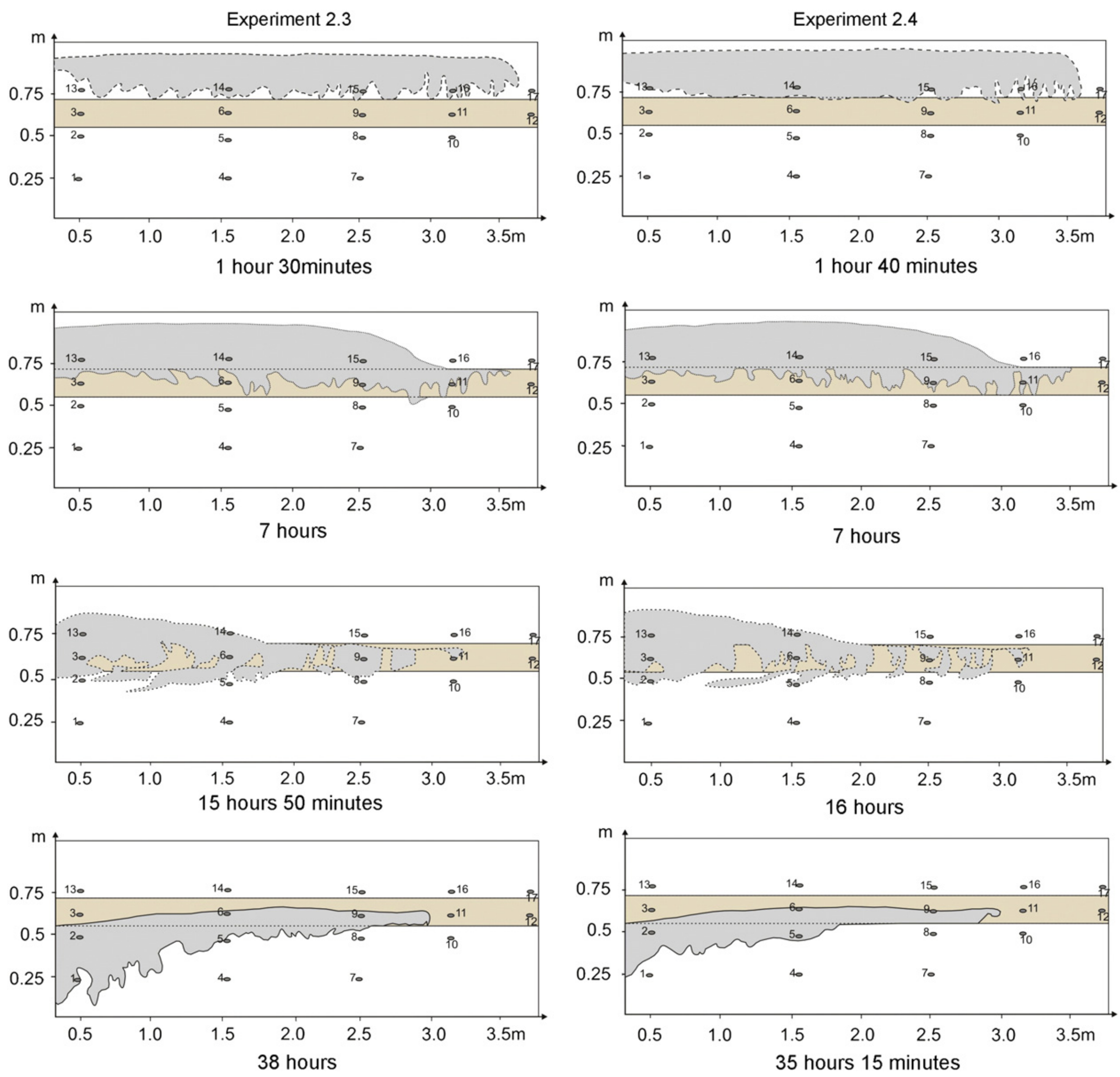


**Fig. 4.** Digitized outlines of plume migration layered Experiments 2.3 (left) and layered Experiments 2.4 (right). Gray area is saltwater plume. Brown area is #70 sand. (For interpretation of the references to color in this figure legend, the reader is referred to the web version of this article.)

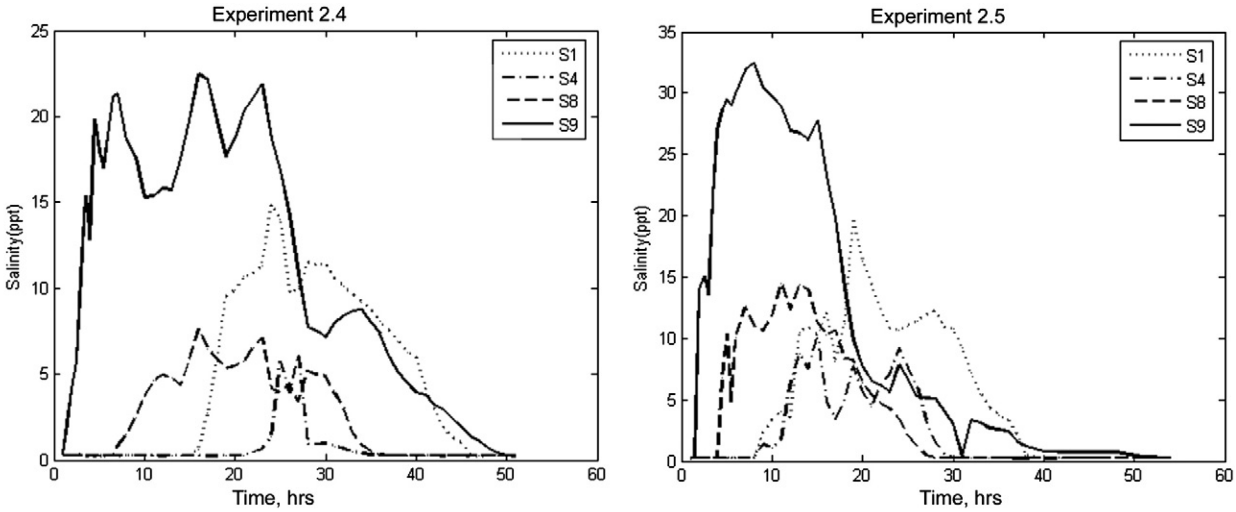


**Fig. 5.** Breakthrough curves obtained from manual water sampling at different sensor locations for Experiments 2.4 (left) and 2.5 (right).

small-scale wave-like instabilities developed at the interface, and these continued to develop along the lower plume boundary with occasional outbreaks of larger fingers. In some cases, the plume showed a kind of quasi-stable behavior right after leaving the low-permeability layer. This behavior might be explained by the sudden change in horizontal flow velocity

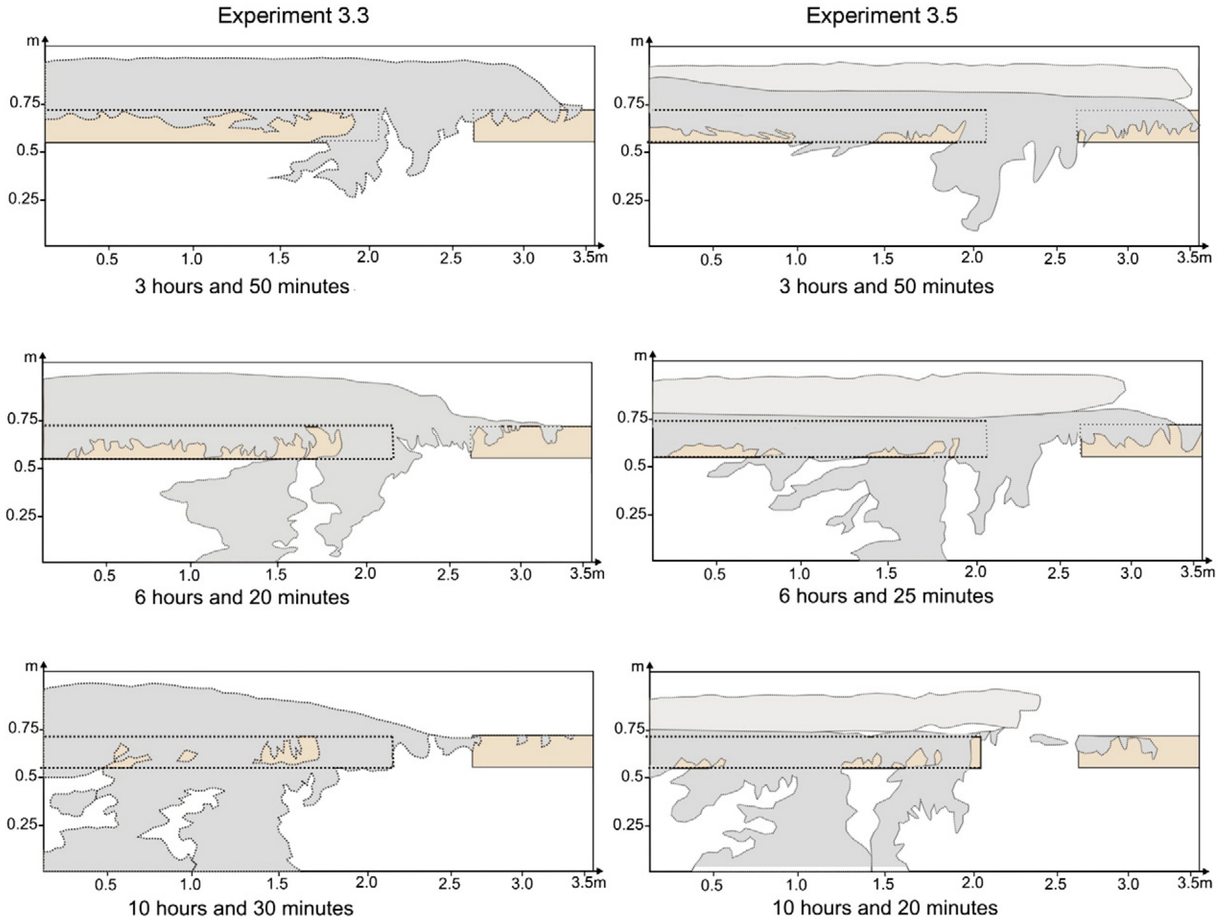


**Fig. 6.** Digitized outlines of plume migration for layered Experiments 3.3 (left, no freshwater recharge) and 3.5 (right, freshwater recharge). Gray area is saltwater plume, light gray is freshwater, and brown is #70 sand. (For interpretation of the references to color in this figure legend, the reader is referred to the web version of this article.)

from the bottom edge of the low-permeability layer to the high permeability layer below.

In Experiment 2.5, which represents rainfall following saltwater contamination after a tsunami, the freshwater pushed the dense saltwater plume downwards and the plume reached greater depths earlier than in Experiment 2.4. This can be seen from the breakthrough curves obtained from manual sampling, for example at S1 and S4 in Fig. 5. In Experiments 2.4 and 2.5 the concentrations are at background values after approximately 46 and 38 h, respectively. The breakthrough curves in the low-permeability layer (S9) illustrate the slow movement and release of the plume from this layer.

The series of experiments in layered experimental configuration II was designed to investigate the effect of a discontinuity in the low-permeability layer on plume behavior. The denser saltwater plume moved quickly down into the lower coarse layer through the opening in the low-permeability layer as shown in Fig. 6. At the same time the salt water infiltrated slowly into the low-permeability layer as fingers and exited the layer in a manner similar to the layered experimental configuration I. As expected, the saltwater plume in the lower part of the tank (with coarse sand) departed the tank quicker than the plume inside the low-permeability layer. Towards the end of the experiments, the plume departing the low-permeability layer showed a stable behavior due to very low density gradient as a result of mixing.

In the case with freshwater flushing (Experiment 3.5) the dense salt water entered more rapidly into the low-permeability layer due to the additional pressure head created by the freshwater flux. The overall behavior of the plume in the high- and low-permeability layers was similar to that of Experiment 3.3. The total flushing time in Experiment 3.5 as compared to the layered configuration I (2.5) was about 28 h longer due to slower movement of salt water inside the low-permeability layer towards the end of the experiment. Differences in boundary conditions may only partially explain this. In Experiment 3.5 more salt water was injected into the tank due to a higher saltwater flux (Table 1), thus it will also take longer to flush out. On the other hand the head drop across the tank was higher in Experiment 3.5, in which everything being equal would lead to a smaller flushing time.

## 5. Results: numerical modeling

The parameter values specified in the numerical model are listed in Table 2. Since the upper part of the tank was repacked for the layered configurations, we expected that the permeability values might be slightly different from that of

**Table 2**
Model parameters used for simulation of tank experiments.

| Fixed parameters | Value |
|---|---|
| Freshwater density $\rho_{min}$ (kg/m$^3$) | 998 |
| Saltwater density $\rho_{max}$ (kg/m$^3$) | 1025 |
| Fluid dynamic viscosity $\mu$ (kg/ms) | 0.001 |
| Molecular diffusion coefficient $D_0$ (m$^2$/s) | $1\times10^{-9}$ |
| Acceleration due to gravity g (m/s$^{-2}$) | 9.81 |
| Model domain | |
| Length (m) | 4.00 |
| Width (m) | 0.05 |
| Depth (m) | 1.10 |
| Number of nodes | |
| X direction | 801 |
| Y direction | 2 |
| Z direction | 221 |
| Total number of nodes | 354,042 |
| Time step | 0.001 min |
| Length of flux application (m) | 2.80 |
| Intrinsic permeability k (m$^2$) | |
| #30: $k_x=k_z$ | $9.0\times10^{-11}-1.1\times10^{-10}$ |
| #70: $k_x=k_z$ | $9.0\times10^{-12}$ |
| Porosity $\varepsilon$ | 0.43 |
| Dispersivity (m) | |
| Longitudinal dispersivity $\alpha_L$ | 0.002 |
| Transverse dispersivity $\alpha_T$ | 0.0002 |

For the modeling, the following equation, available in HST3D was used for calculating density as a function of solute mass fraction: $\rho(w)=\rho_0+[\rho(w_{max})-\rho(w_{min})]*(w-w_{min})/(w_{max}-w_{min})$ with the following values: $w_{max}=0.0357$; $w_{min}=0$; $\rho_0=998.23$ kg/m$^3$; $\rho(w_{max})=1030$ kg/m$^3$; and $\rho(w_{min})=998.23$. w is the simulated mass fraction at a particular point.

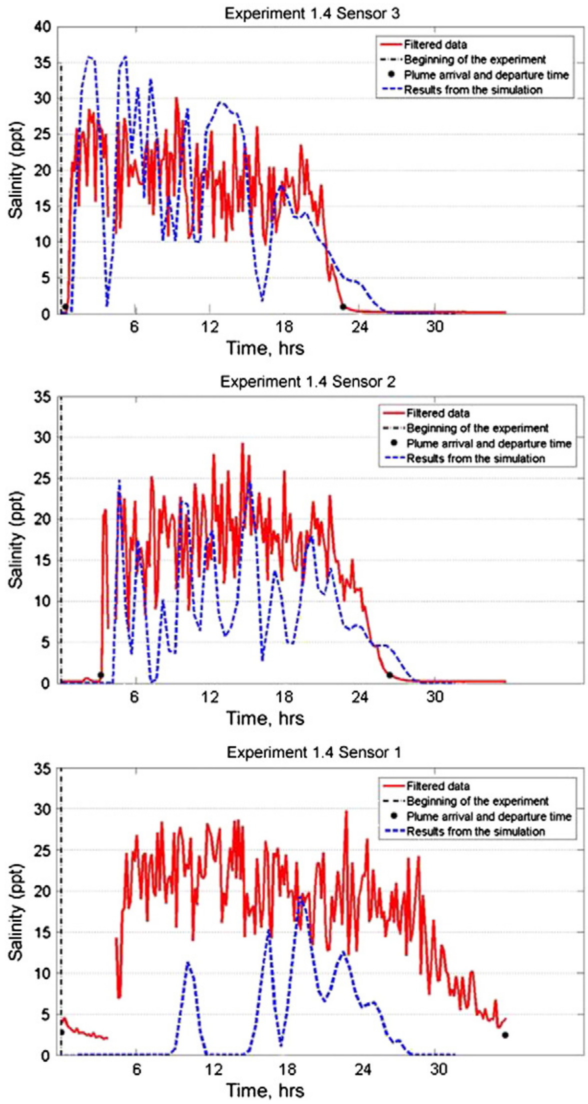


**Fig. 7.** Filtered observed and simulated breakthrough curves, Experiment 1.4.

the homogeneous configuration. First HST3D was calibrated manually for Experiment 1.3 using the plume departure time as the calibration target leading to a permeability value (k) of $9.0\times10^{-11}$ $m^2$ for #30 sand. This value is a factor of ~2.25 lower than the measurements obtained in sand column experiments. Such a reduction was considered reasonable given that the tank and the column necessarily could not be packed exactly to same compaction level. This k value was used for the homogeneous packing and for the #30 sand located below the low-permeability layer of the layered configurations. For the upper #30 sand layer, a slightly higher value of $1.1\times10^{-10}$ $m^2$ was specified in order to obtain the same plume migration time as in the experiment. After packing of the low-permeability layer, the top coarse layer was not packed as tightly as in the homogeneous configuration due to constraints in tapping the sand in the top layer. This leads to a slightly higher permeability. The results from the column experiments showed that the permeability of #70 sand was one order of magnitude less than the value for #30 sand. In the model simulations we assumed this ratio was applicable.

Initial model simulations showed that the simulated pattern and migration of the solute plume are highly sensitive to the dispersivity values. Simulation results of the homogeneous

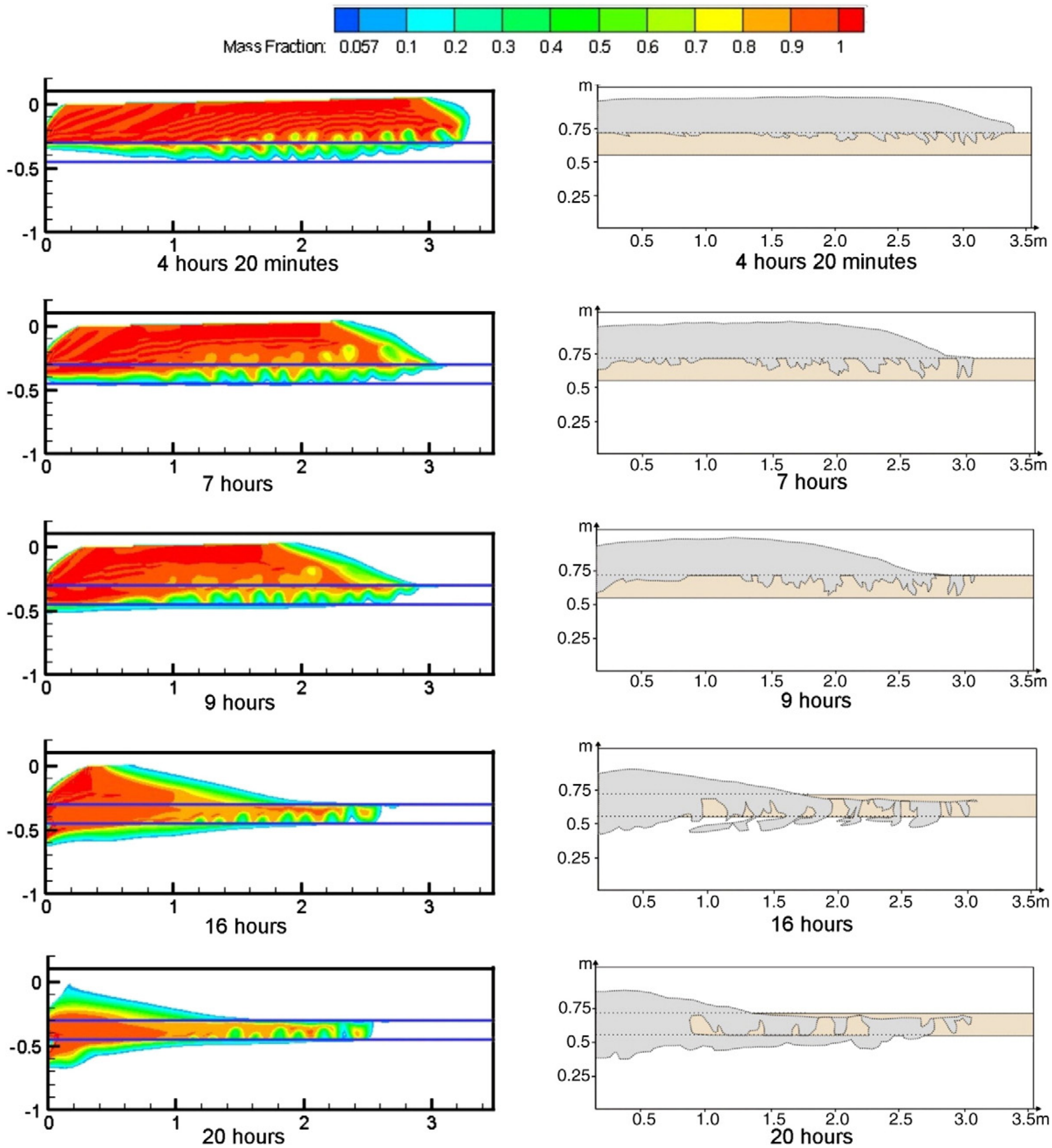


**Fig. 8.** Simulated scaled mass fractions (left) and observed outline of plume (right) for Experiment 2.4. Brown area is #70 sand. (For interpretation of the references to color in this figure legend, the reader is referred to the web version of this article.)

Experiment 1.3 are presented in Fig. 3 (left pane) using $\alpha_L = 2$ mm, which was found through a series of sensitivity tests to give the best match of observed plume spreading. Wiggles were generated in the simulated plume profiles due to the spacing between the drippers. This is clear from Fig. 3, where exactly 10 wiggles are present. Wiggles, however, were also generated as a result of numerical errors (under- and overshoot), which can be seen in Fig. 7 that shows measured and simulated breakthrough curves for Experiment 1.4. Experimental breakthrough curves also show high frequency concentration fluctuations, which are partly due to remaining sensor noise, but also caused by salt fingers moving through the tank. These were also seen visually inside the plumes (Fig. 2). The simulation results are subject to fewer but higher fluctuations than the observations. We are not sure why this is the case. A good overall match between measurements and simulations was obtained for sensors close to the source zone (#3, #6 and #9) and in the middle part of the tank (#2, #5 and #8), while the model tended to underestimate the concentrations for sensors located deeper in the tank (#1, #4 and #7). The most conspicuous discrepancy between the model and data is caused by the model's inability to capture the high-

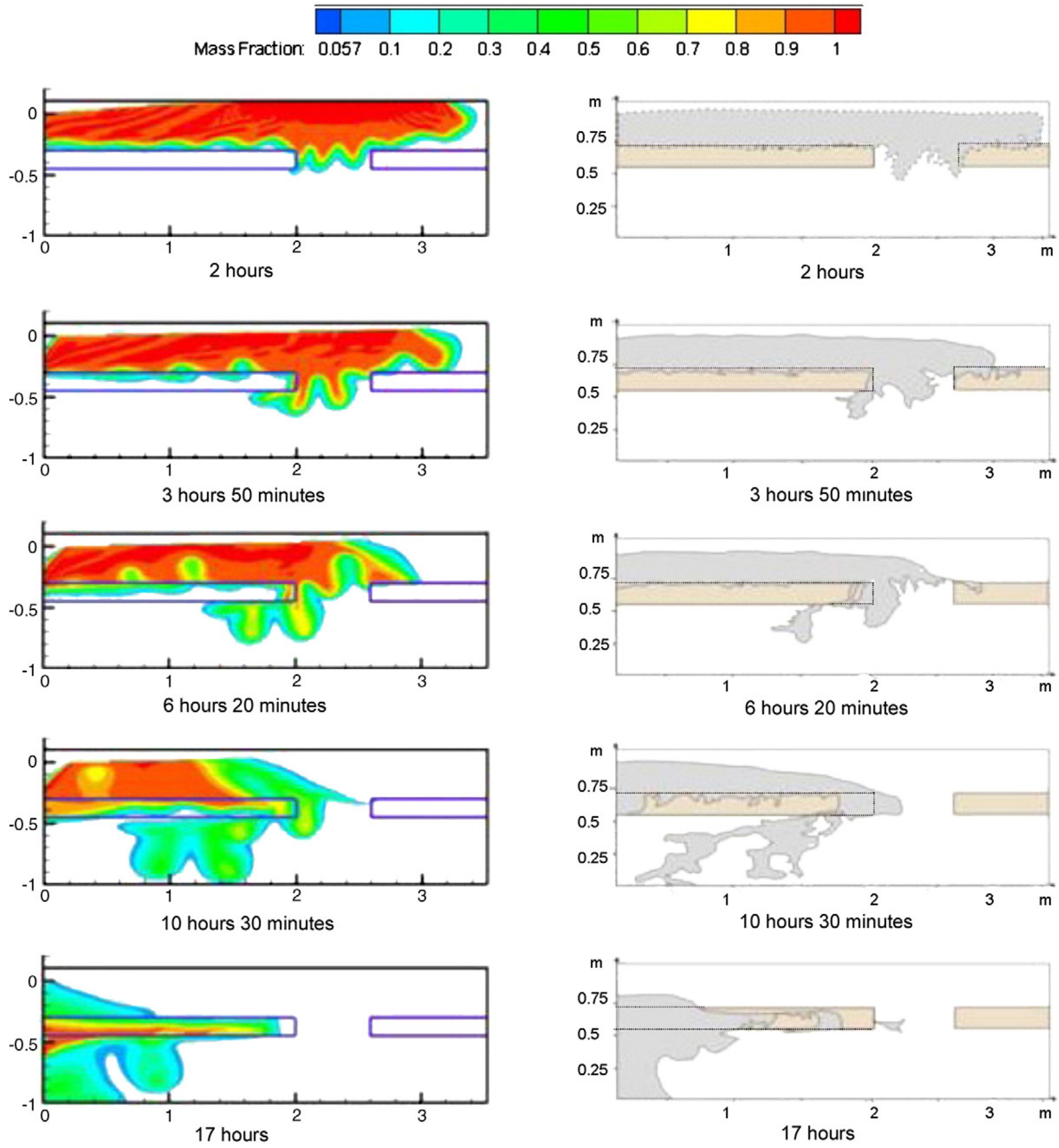


**Fig. 9.** Simulated scaled mass fractions (left) and observed outline of plume (right) for Experiment 3.4. Brown area is #70 sand. (For interpretation of the references to color in this figure legend, the reader is referred to the web version of this article.)

frequency instabilities. This is likely caused by the lack of inclusion of micro-scale K variability plus numerical dispersion that dampens instabilities. The results demonstrate the difficulties in obtaining accurate predictions under unstable conditions.

Simulation of Experiment 1.5 (with the application of freshwater after the saltwater injection), matched observations well (not shown here). No instabilities were observed in the freshwater plume boundary indicating less mixing between waters with different densities.

The simulations of the layered experimental configuration I gave a good fit of both plume pattern and migration time, shown for Experiment 1.4 in Fig. 8. When the plume reached the low-permeability layer, several small intruding gravitational instabilities were present both in observations and simulations. The opposite occurred when the plume moved into the underlying high-permeability layer, where forced convection was more dominant.

The simulations for the layered configuration II with an opening in the low-permeability layer also showed a good agreement with the observations (Experiment 3.4) as shown in Fig. 9. As in the experiment, part of the simulated plume penetrated through the opening to the bottom of the tank and was flushed out more quickly than the salt water in the low-permeability layer. The simulations for the case with freshwater application on the top of the saltwater plume (Fig. 10) also compare reasonably well with the experimental observations. Particularly, the residual salt water in the small low-permeability block at the right hand end of the tank was also present in the simulations.

### 5.1. Simulation of flush-out times

The model was used to simulate flush-out times for the different porous media configurations and to explore the effects on freshening of the system by applying the freshwater flux after injection of salt water. The different simulations were conducted under identical conditions: permeability for #30 sand $9.0\times10^{-11}$ m$^2$ and for #70 sand $9.0\times10^{-12}$ m$^2$; the same ambient flow rate; the same saltwater flux rate of $4.0\times10^{-5}$ m/s with an application time of 2 h; and the same freshwater flux rate with an application time of 1 h starting 1 h after the saltwater application ended.

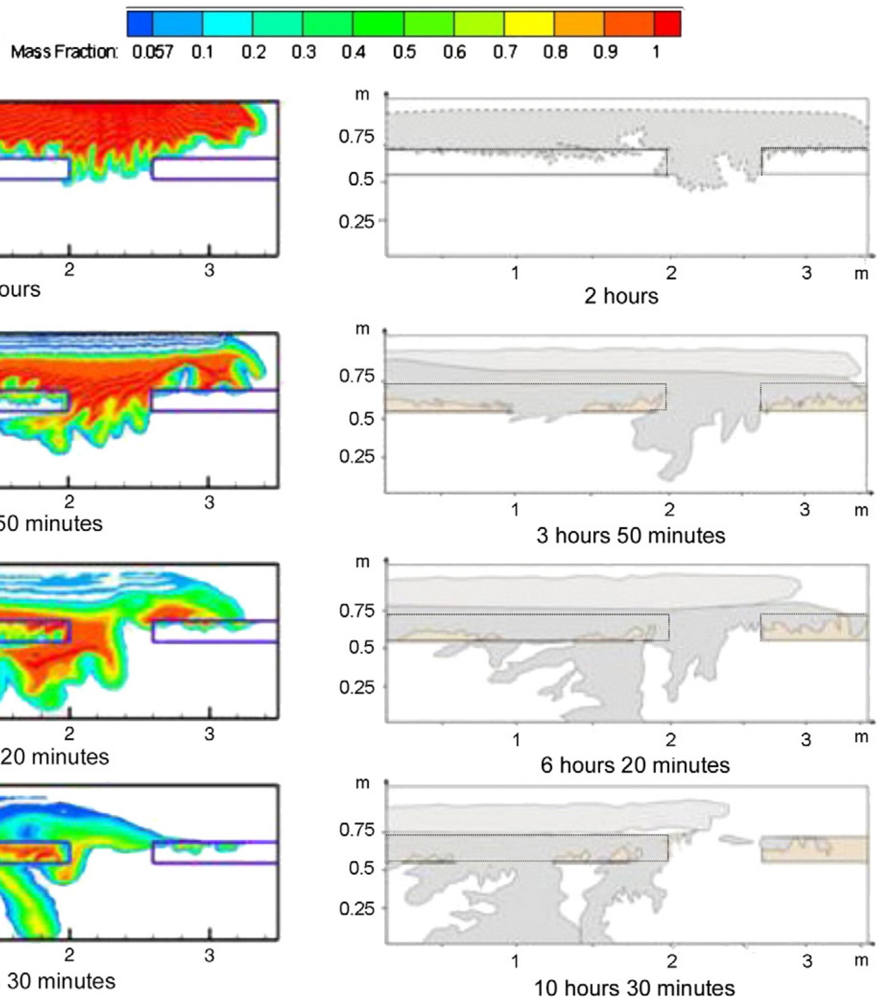


**Fig. 10.** Simulated scaled mass fractions (left) and observed outline of plume (right) for Experiment 3.5 with freshwater application after saltwater flux. Brown area is #70 sand. (For interpretation of the references to color in this figure legend, the reader is referred to the web version of this article.)

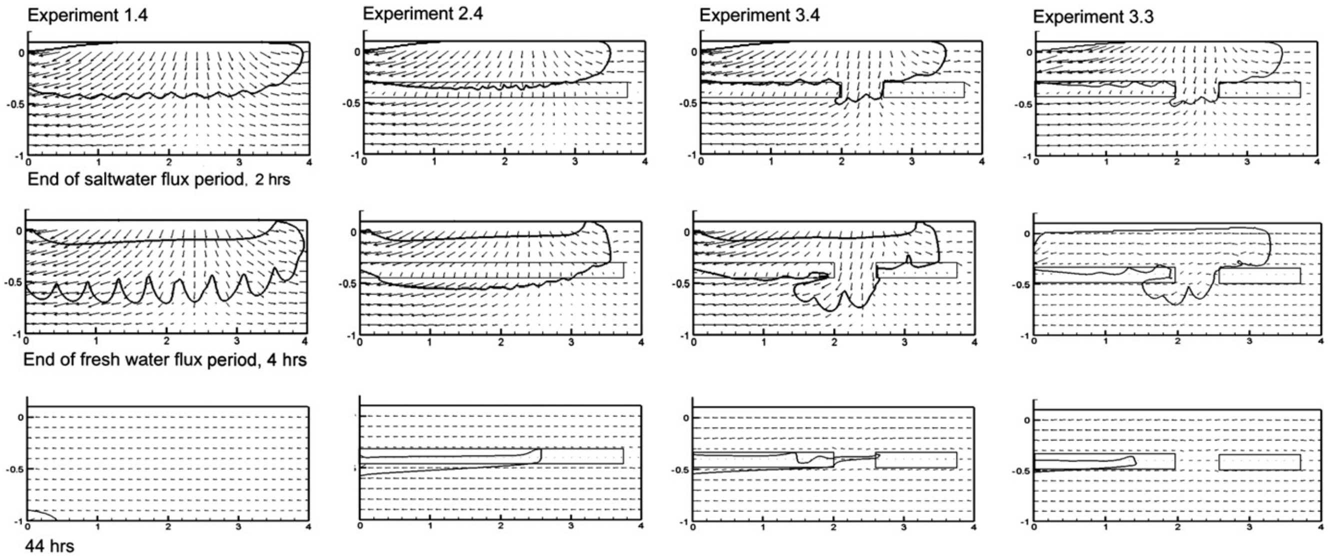


**Fig. 11.** Plume contours at various times for the different system configurations.

Fig. 11 shows the simulation results for the three systems considered in the study. The plume outlines are shown by the 0.02 mass fraction contour line at three different times; at the end of the saltwater application period (2 h), at the end of the freshwater application period (4 h), and after 44 h, which represents almost complete flushing of the salt water in the system. A mound was created in all cases due to the injection of salt water and freshwater. When the freshwater flux stopped, the flow returned to ambient conditions. During the period with a mound, salt water moved opposite to the direction of ambient flow. Significantly different flow and transport patterns were obtained when a low-permeability layer was present in the system. First of all, the flushing of the salt water was slower with the presence of the low-permeability layer, simply because salt water flowed slowly in this layer. After 44 h the low-permeable layer still contained a significant amount of salt water. A small opening in the low-permeability layer caused a more rapid flushing of the salt water, because, as shown for example after 4 h, part of the salt water migrated through the window to the higher permeability layer below. The low-permeability layer also reduced the magnitude of the instabilities; these were much more prominent in the homogeneous configuration. It is also clear that the presence of a low-permeability layer caused the salt water to stay in the shallow part of the system much longer compared to the homogeneous configuration. These results demonstrate that geological heterogeneity (layering) of a coastal aquifer has a strong influence on the length of time it takes to return to pre-tsunami conditions following flooding by salt water.

Fig. 12 shows the cumulative salt mass outflow ratio as a function of time. Cumulative mass outflow has been normalized by the total salt mass applied to the system. All simulations reached a ratio of one showing good model mass balance. Complete flush-out was achieved after approximately 32 h in the homogeneous configuration with freshwater recharge, which is close to 40% faster than for the layered configurations I and II. Flushing of the first part of the salt water (about 60%) was, however, achieved in more or less the same time period for the different configurations. The difference in the total flushing time between the scenarios was mainly caused by a slower movement of the salt water in the low-permeability layer.

The simulation results for the salt mass outflow in the homogeneous configuration showed a smooth behavior

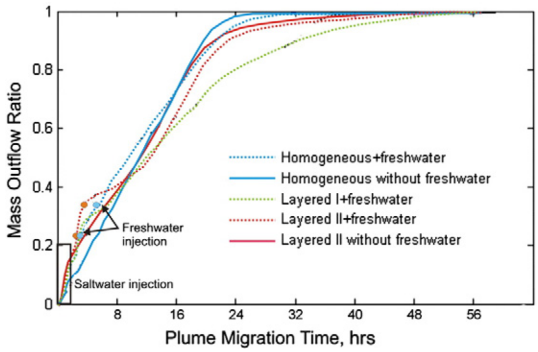


**Fig. 12.** Cumulative solute mass outflow ratio for the different system configurations.

throughout the experiment, while for both layered configurations some fluctuations occurred particularly during freshwater recharge. Freshwater recharge enhanced an early flush-out of salt water from the upper high-permeability sand layer in both layered configurations (Fig. 12). However, the freshwater recharge increased the total flush-out time because of the extra salt water that was pushed into the low-permeability layer, visible as the residual salt water in Fig. 11. Nevertheless, freshwater recharge could lead to a more rapid improvement in water quality for the communities that extract groundwater from the shallow depths of the aquifer.

It took about 50 h to flush-out a one-hour application of salt water. The time for total flushing was controlled primarily by the ambient flow rate (the flow situation after 4 h). The ambient flow rate used in the physical experiments was about 100–200 times higher than typical values under field conditions. This suggests that it could take tens of years to achieve complete flush-out in field systems, which is in agreement with similar studies (Anderson and Lauer, 2008).

## 6. Summary and conclusions

Flushing of salt water from freshwater aquifers affected by sea water flooding is one of the most important considerations for the recovery in the aftermath of a major tsunami such as the one which occurred in December 2004 in Asia. This is important for many coastal communities that depend on the freshwater resources, which are normally sustained by regional groundwater flow and local recharge from rainfall.

We conducted sand tank experiments to mimic a tsunami type event in the field. We combined chemical and visual observations of the experiments with numerical model simulations to investigate the fate and migration of inundating saline water and the recovery of the aquifer during subsequent recharge by freshwater.

The study resulted in several important major conclusions. First, it is evident that subsurface heterogeneity plays a critical role in determining both the extent of salinization and the time of recovery. The migration path of the plume and the flushing time are significantly influenced by the nature of the heterogeneity indicating that the knowledge of the hydrostratigraphy of freshwater aquifers affected by tsunami flooding is extremely important. Second, the addition of freshwater recharge either due to rainfall or by artificial means leads to a rapid improvement in the quality of water. However, it was found that the freshwater addition may increase the total flush-out time if the salt water is pushed into the low-permeability lenses. Third, it was demonstrated that the numerical model used in this study is capable of simulating the overall plume migration patterns and flushing times for various porous media configurations, saltwater application, ambient flow, and freshwater application. However, careful attention is needed to control the numerical errors in simulations as they could manifest themselves as unrealistic plume patterns.

## Acknowledgments

The first author would like to thank colleagues in CESEP laboratory (Center for Experimental Study of Subsurface

Environmental Processes) at Colorado School of Mines and Rohit Goswami and Prabhakar Clement from Auburn University for their kind support and advice to the tank experiments. Thanks go to Peer Jørgensen, University of Copenhagen, Colin Campbell and Doug Cobos, Decagon Devices Inc. for their assistance during the laboratory experiments. Craig Simmons provided important suggestions on modeling, and Kenneth Kipp, Karen Villholth and the International Water Management Institute (IWMI) are kindly acknowledged for their valuable assistance given. We would like to express our sincere appreciation to the editor and reviewers for their insightful comments. These comments have been very useful and have certainly helped in improving the manuscript.

## References

Andersen, M.S., Nyvang, V., Jakobsen, R., Postma, D., 2005. Geochemical processes and solute transport at the seawater/freshwater interface of a sandy aquifer. Geochimica et Cosmochimica Acta 69, 3979–3994.

Anderson Jr., W.P., Lauer, R.M., 2008. The role of overwash in the evolution of mixing zone morphology within barrier islands. Hydrogeology 16, 1483–1495.

Barth, G.R., Hill, M.C., Illangesekare, T.H., Rajaram, H., 2001. Predictive modeling of flow and transport in a two-dimensional intermediate-scale, heterogeneous porous medium. Water Resources Research 37 (10), 2503–2512.

Carlson, D.A., Van Biersel, T.P., Milner, L.R., 2008. Storm-damaged saline-contaminated boreholes as a means of aquifer contamination. Ground Water 46, 69–79.

Diersch, H.J., 1988. Finite element modeling of recirculating density driven saltwater intrusion processes in groundwater. Advances in Water Resources 11 (1), 25–43.

Diersch, H.-J.G., Kolditz, O., 2002. Variable-density flow and transport in porous media: approaches and challenges. Advances in Water Resources 25, 899–944.

Fan, Y., Kahawita, R., 1994. A numerical study of variable density flow and mixing in porous media. Water Resources Research 30 (10), 2707–2716.

Frippiat, C.C., Perez, P.C., Holeyman, A.E., 2008. Estimation of laboratory scale dispersivities using an annulus-and-core device. Journal of Hydrology 362, 57–68.

Goswami, R.R., Clement, T.P., 2007. Laboratory scale investigation of saltwater intrusion dynamics. Water Resources Research 43, W04418.

Guvanasen, V., Volker, R.E., 1983. Numerical solutions for solute transport in unconfined aquifers. International Journal for Numerical Methods in Fluids 3, 103–123.

Hayworth, J.S., 1993. A physical and numerical model study of three dimensional behaviour of dense aqueous phase contaminant plumes in porous media, Doctoral Thesis, Department of Civil Engineering. Auburn University, Alabama.

Huyakorn, P.S., Pinder, G.F., 1983. Computational Methods in Subsurface Flow. Academic Press, Inc., NY. 473 pp.

Illangasekare, T., Tyler, S.W., Clement, T.P., Villholth, K.G., Perera, A.P.G.R.L., Obeysekera, J., Gunatilaka, A., Panabokke, C.R., Hyndman, D.W., Cunningham, K.J., Kaluarachchi, J.J., Yeh, W.W.G., Van Genuchten, M.R., Jensen, K.H., 2006. Impacts of the 2004 tsunami on groundwater resources in Sri Lanka. Water Resources Research 42, W05201.

Kipp Jr., K.L., 1987. A computer code for the simulation of heat and solute transport in three-dimensional groundwater flow systems. Water Resources Investigations Report 86–4905 (1–517 pp., U.S. Geol. Surv.).

Koch, M., Zhang, G., 1992. Numerical simulation of the effects of variable density in a contaminant plume. Ground Water 30 (5), 731–742.

Langevin, C.D., Guo, W., 2006. MODFLOW/MT3DMS-based simulation of variable density groundwater flow and transport. Ground Water 44 (3), 339–351.

Liu, H.H., 1995. An experimental and numerical study on flow and mixing of variable density fluids in porous media, Doctoral Thesis, Department of Agronomy and Soil Science. Auburn University, Alabama.

Liu, H.H., Dane, J.H., 1996. A criterion for gravitational instability in miscible dense plumes. Journal of Contaminant Hydrology 23, 233–243.

Moazed, H., Maroufpour, E., Kashkouli, H.A., Samani, J.M.V., 2009. Laboratory scale effect of aquifer thickness on dispersivity of porous media. Journal of Applied Sciences 9 (3), 542–548.

Oostrom, M., Hayworth, J.S., Dane, J.H., Güven, O., 1992a. Behavior of dense aqueous phase leachate plumes in homogeneous porous media. Water Resources Research 28 (8), 2123–2134.

Oostrom, M., Dane, J.H., Güven, O., Hayworth, J.S., 1992b. Experimental investigation of dense solute plumes in an unconfined aquifer model. Water Resources Research 28 (9), 2315–2326.

Oswald, S.E., Kinzelbach, W., 2004. Three-dimensional physical benchmark experiments to test variable density flow models. Journal of Hydrology 290, 22–42.

Oude Essink, G.H.P., 1998. MOC3D adapted to simulate 3D density-dependent groundwater flow. Proc. MODFLOW'98 Conf., Golden, Colorado, USA, pp. 291–303.

Post, V.A.E., Simmons, C.T., 2010. Free convective controls on sequestration of salts into low permeability strata: insights from sand tank laboratory experiments and numerical modelling. Hydrogeology Journal 18, 39–54.

Prasad, A., Simmons, C.T., 2003. Unstable density driven flow in heterogeneous porous media: a stochastic study of the Elder (1967b) 'short heater' problem. Water Resources Research 39 (1), 1007, http://dx.doi.org/10.1029/2002WR001290.

Sakaki, T., Illangasekare, T.H., 2007. Comparison of height-averaged and point-measured capillary pressure–saturation relations for sands using a modified Tempe cell. Water Resources Research, http://dx.doi.org/10.1029/2006WR005814.

Sanford, W.E., Konikow, L.F., 1985. A two-constituent solute-transport model for groundwater having variable density. Water Resources Investigations Report (United States Geological Survey) 85–4279.

Schincariol, R.A., Schwartz, F.W., 1990. An experimental investigation of variable density flow and mixing in homogeneous and heterogeneous media. Water Resources Research 26 (10), 2317–2329.

Schincariol, R.A., Hederick, E.E., Schwartz, F.W., 1993. On the application of image analysis to determine concentration distributions in laboratory experiments. Journal of Contaminant Hydrology 12, 197–215.

Simmons, C.T., Narayan, K.A., 1997. Mixed convection processes below a saline disposal basin. Journal of Hydrology 194, 263–285.

Simmons, C.T., Narayan, K.A., Wooding, R.A., 1999. On a test case for density-dependent groundwater flow and solute transport models: the salt lake problem. Water Resources Research 35 (12), 3607–3620.

Simmons, C.T., Pierini, M.L., Huston, J.L., 2002. Laboratory investigation of variable density flow and solute transport in unsaturated–saturated porous media. Transport in Porous Media 47, 215–244.

Swartz, C.H., Schwartz, F.W., 1998. An experimental study of mixing and instability development in variable density systems. Journal of Contaminant Hydrology 34, 169–189.

Terry, J.P., Falkland, A.C., 2010. Responses of atoll freshwater lenses to storm-surge overwash in the Northern Cook Islands. Hydrogeology Journal 18 (3), 749–759, http://dx.doi.org/10.1007/s10040-009-0544-x.

Vithanage, M. 2009. Effect of tsunami on groundwater; Field studies and tank experiments. Doctoral Thesis, Department of Geography and Geology. University of Copenhagen, Denmark.

Vithanage, M., Villholth, K.G., Mahatantila, K., Engesgaard, P., Jensen, K.H., 2009. Effect of well cleaning and pumping on groundwater quality of a tsunami-affected coastal aquifer in eastern Sri Lanka. Water Resources Research, http://dx.doi.org/10.1029/2008WR007509.

Voss, C.I., 1984. SUTRA: a finite-element simulation model for saturated unsaturated fluid density-dependent groundwater flow with energy transport or chemically reactive single-species solute transport. Water Resources Investigations Report (United States Geological Survey) 84–4369.

Wooding, R.A., Tyler, S.W., White, I., 1997a. Convection in groundwater below an evaporating salt lake: 1. onset of instability. Water Resources Research 33 (6), 1199–1217.

Wooding, R.A., Tyler, S.W., White, I., Anderson, P.A., 1997b. Convection in groundwater below an evaporating salt lake: 2. evolution of fingers or plumes. Water Resources Research 33 (6), 1219–1228.

Zhang, Q., Volker, R.E., Lockington, D.A., 2002. Experimental investigation of contaminant transport in coastal groundwater. Advances in Environmental Research 6, 229–237.